Geomorphology 474 (2025) 109648

Contents lists available at ScienceDirect

Geomorphology

journal homepage: www.journals.elsevier.com/geomorphology

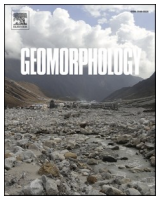

Cosmogenic dating reveals the timing of glaciers collapse in the high Dolomites valleys (Northern Italy)

Carlo Baroni [a,b], Maria Cristina Salvatore [a,b], Vittoria Vandelli [c,*], Mauro Marchetti [d], ASTER Team [e,1], Mauro Soldati [c]

[a] Dipartimento di Scienze della Terra, University of Pisa, Via Santa Maria, 53, 56126 Pisa, Italy
[b] CNR-IGG, Istituto di Geoscienze e Georisorse, Pisa, Italy.
[c] Dipartimento di Scienze Chimiche e Geologiche, University of Modena and Reggio Emilia, Via Campi 103, 41125 Modena, Italy
[d] Dipartimento di Educazione e Scienze Umane, University of Modena and Reggio Emilia, Viale Allegri 9, 42121 Reggio Emilia, Italy
[e] Aix Marseille University, CNRS, IRD, INRAE, CEREGE, Aix-en-Provence, France

ARTICLE INFO

Keywords:
Glacial geomorphology
ELA reconstruction
Deglaciation
Lateglacial
^{36}Cl cosmogenic nuclides
Italian Dolomites

ABSTRACT

During the Last Glacial Maximum (LGM) the Italian Alps were extensively ice-covered with icefields feeding a network of interconnected valley glaciers and piedmont glaciers spilling into the foreland. The subsequent Lateglacial ice retreat occurred with different modes and timing across the region. This paper arises from the need for further investigation to better understand the glaciers' dynamics of the period and focuses on the glacial history of the Alta Badia valley (Eastern Dolomites, Italian Alps) as a key area for reconstructing the LGM glaciers' collapse and Lateglacial readvances within the region. We present a reconstruction of LGM and Lateglacial glaciers' evolution supported by cosmogenic ^{36}Cl surface exposure data - obtained for the first time in the area - and geomorphological evidence. Our findings suggest that LGM ice retreat began before 17 ka BP. Within a general trend of ice decay, we identified the Gschnitz readvance from reconstructed glacier surfaces and Equilibrium Line Altitude (ELA) estimates, supported by moraine dating (15.8–15.4 ka BP) in the southeastern sector of the valley. Similarly, a Lateglacial readvance corresponding to the traditional Daun Readvance was recognized in the southwestern sector, based on exposure ages (14.4 and 13.3 ka BP) and calculated ELA. Evidence indicates that after the Daun phase, the valley was nearly deglaciated, retaining only small glacial remnants at higher elevations. This study enhances our understanding of LGM ice retreat and Lateglacial chronology, providing insights into the Alpine glacial history and establishing a foundation for estimating paleoclimatic conditions of the region.

1. Introduction

The Last Glacial Maximum (LGM), corresponding to Marine Isotope Stage 2 (MIS 2) and also known as the Würmian Pleniglacial (26.5–19 ka BP) represents the peak of the last Ice Age (Clark et al., 2009).

The subsequent transition from glacial to interglacial conditions, known as Termination I (ca. 20–8 ka BP), marks one of the most significant climate changes in Earth's history (Paillard, 2009). This period is characterized by increasing global temperature, rising global sea levels, and widespread ice-sheet retreat (Clark et al., 2012; Marcott et al., 2013). Despite its global significance key questions remain unsolved about the drivers, and regional dynamics of this transition.

The Alps and their foreland constitute a key region for the study of glacier dynamics during the LGM and the Termination I. Several moraine systems in valleys and glacial cirques document the Alpine Lateglacial stadials, somehow reflecting the sequence of interstadials and stadials recorded in Greenland profiles with robust correlation between different proxy climate records (cf. INTIMATE project - INTegrating Ice-core, MArine, and TErrestrial records in Rasmussen et al., 2014).

The LGM in the European Alps is well constrained between 26.5 and 19 ka BP (e.g., Ivy-Ochs et al., 2008; Ivy-Ochs, 2015; Rossato and Mozzi, 2016; Wirsig et al., 2016; Monegato et al., 2017; Bernsteiner et al., 2021 and references therein). After the LGM peak, Alpine valley glaciers

* Corresponding author.
E-mail address: vittoria.vandelli@unimore.it (V. Vandelli).
[1] ASTER Team: Georges Aumaître, Karim Keddadouche, Fawzi Zaidi.

https://doi.org/10.1016/j.geomorph.2025.109648
Received 4 December 2024; Received in revised form 3 February 2025; Accepted 4 February 2025
Available online 6 February 2025

underwent a general decline, decreasing in volume and withdrawing from the forelands. Stagnant remnants of the former ice-stream network experienced downwasting in the major valleys, while separate valley and cirque glaciers of the higher tributary valleys readvanced during progressively minor glacier advances known as Lateglacial stadials (Ivy-Ochs et al., 2023 and references therein). Despite the availability of these records, the exact timing of glacier fluctuations remains debated, highlighting the need for more precise chronological constraints. In the Eastern Alps, three Lateglacial stages are currently recognized, namely: (i) the early Lateglacial phase of ice retreat (19–18 ka BP); (ii) the Gschnitz stadial (17–16 ka BP); and (iii) the Egesen stadial (13–11.5 ka) (Ivy-Ochs et al., 2023 and references therein). On the other hand, little information is available about the behaviour of stagnant ice within valleys and basins of the inner Alpine chain.

The Gschnitz stadial was the most significant one and it is witnessed by well-developed frontal and lateral moraines located in the main Alpine valleys. ^{10}Be exposure dating of stadial moraines in the Gschnitz type locality (Austria) revealed ages between 17 and 16 ka BP, with an ELA depression of 600–700 m lower than the relative to the Little Ice Age (LIA) ELA (Ivy-Ochs et al., 2006). The Egesen stadial is also well-documented by moraines marking multiple stillstands during the glacial recession (Ivy-Ochs et al., 2023 and references therein) and is associated with the Younger Dryas cold period (12.9–11.7 ka BP). The ELA depression with respect to the LIA ELA is between 250 and 350 m. For instance, Federici et al. (2008) in the Maritime Alps found an ELA depression with respect to the LIA of 260–320 m and 520–530 m compared to the present-day one. In the Austrian and Swiss Alps Kerschner et al. (2000) reported a difference in elevation between the Egesen ELA and the present-day ELA of 450 m near the northern and western margins, and of 300 m in the central valleys.

It is likely that the timing of Lateglacial advances was not fully synchronized across the Alps, as local factors like climate conditions and topography played a role. To gain a deeper understanding of these variations, studies conducted at a local scale across the entire Alpine chain are crucial. These investigations must be underpinned by a robust chronological framework to ensure accurate interpretation of glacier dynamics and regional differences.

In the Alta Badia valley (Autonomous Province of Bolzano, Eastern Dolomites, Italy) evidence of past glacier fluctuations is preserved as recognizable landscape features, despite the strong human imprint and intense slope dynamics. Previous studies attributed those features to the LGM and to the Lateglacial periods based on relative chronology (Mutschlechner, 1932, 1933; Castiglioni, 1964; Panizza et al., 2011; Ghinoi and Soldati, 2017; Vandelli et al., 2019). However, knowledge gaps remain, particularly regarding the timing of deglaciation. In light of the information available in the literature and considering the existing knowledge gaps, this study represents the first ^{36}Cl-based Cosmic Ray Exposure (CRE) dating of glacial deposits in this region. This method was combined with a reconstruction of the Equilibrium Line Altitude (ELA) of former glacier surfaces, providing a detailed framework for understanding glacier dynamics.

The aim of this paper is to define mode and timing of LGM glacier

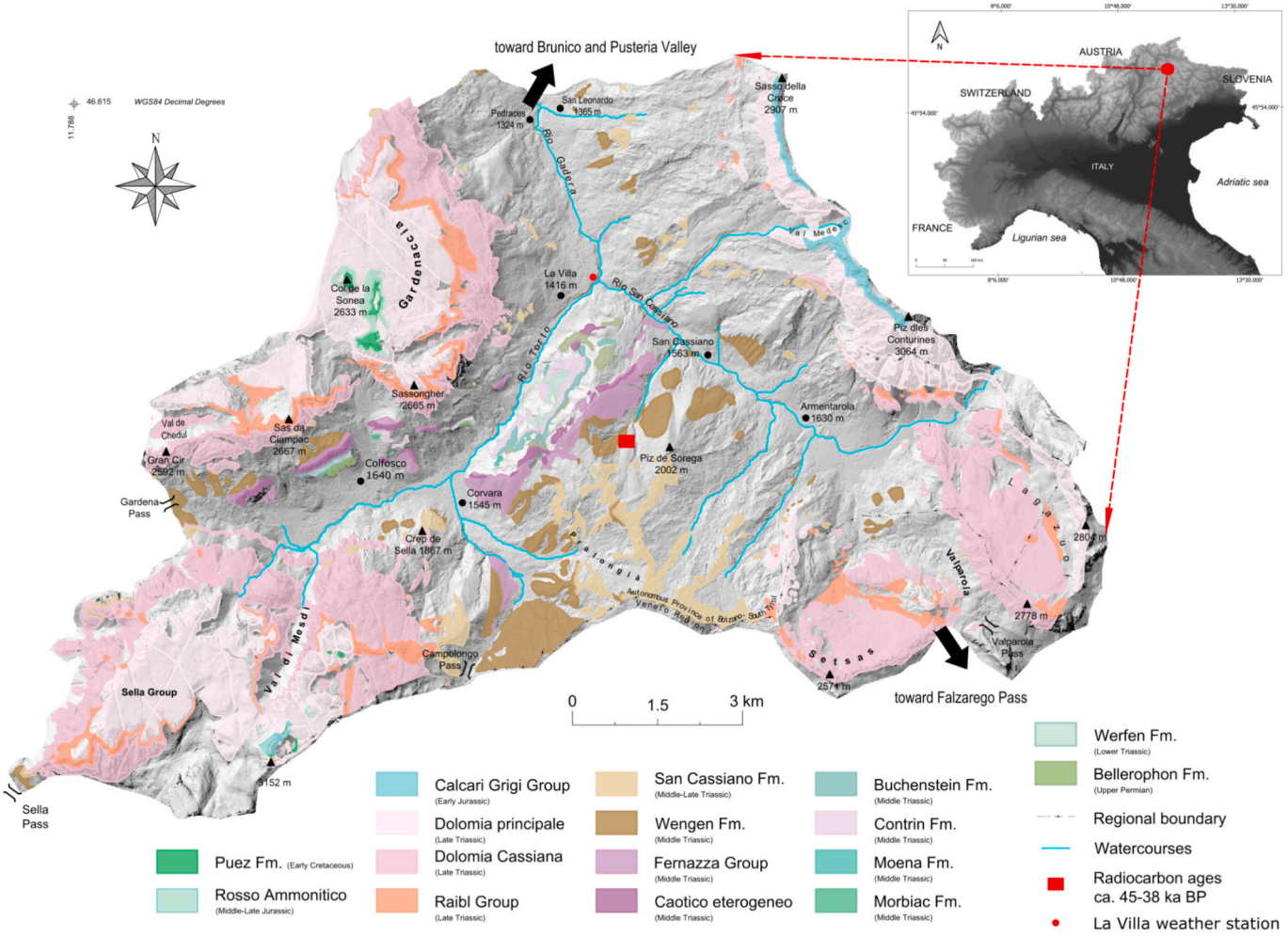

Fig. 1. Geological setting of the Alta Badia valley (LiDAR data courtesy of Servizio cartografia provinciale e coordinamento geodati, Autonomous Province of Bolzano). Quaternary deposits are depicted as uncoloured grey areas.

collapse, the role of local morphology in driving the deglaciation, and possibly to constrain the earlier phases of the Lateglacial advances in this part of the Eastern Dolomites. Additionally, this study seeks to extend the dataset on the glacial geochronology of the Alps by providing further insights, from a high-Alpine perspective, on paleoenvironmental and paleoclimatic conditions occurred during Late Pleistocene in the Eastern Dolomites, as a southern distal part of the Alpine chain.

2. Study area

The study area comprises the Alta Badia valley and a stretch of the Upper Gardena Valley at Sella Pass (Eastern Alps; Fig. 1). It is located in the southern sector of the Eastern Italian Dolomites mainly within the Autonomous Province of Bolzano and secondarily within the Belluno Province (Veneto Region). Elevation ranges between ca. 1300 and 3100 m a.s.l. The study area is bounded by towering Dolomite mountain groups: to the west, the Gardenaccia Group with its highest peaks Sas da Ciampac (2667 m a.s.l.) and Sassongher (2665 m a.s.l.); to the east, the Conturines Group including Piz Lavarela (3055 m a.s.l.) and Piz dles Conturines (3064 m a.s.l.); to the south-west, the Sella Group including Piz Boè (3152 m a.s.l.), the highest peak in the area. Finally, Setsas (2138 m a.s.l.) and Lagazuoi (2752 m a.s.l.) mountains bound the valley to the south-east.

The Alta Badia valley is included within the River Adige catchment. The main water courses are Rio Torto flowing from south-west to north-east and Rio San Cassiano flowing from south-east to north-west. Rio Torto is named Rio Gadera once overpasses the village of Corvara and continues toward the north after the confluence with Rio San Cassiano. The latter are mainly located at the contact between deeply fractured dolomite rocks and the underlying marly and clayey rocks, at a mean altitude of 2000 m. The climate is humid continental with warm summers (Dfb, according to Peel et al., 2007). The mean annual precipitation recorded between the period 1987–2023 at the meteorological station of La Villa (see Fig. 1 for location) is 902 mm and the mean annual temperature is 5.7 °C (Fig. 2). The coldest month is usually January (mean temperature of −4.4 °C), the warmest is July (mean temperature of 15.3 °C). Winter months (December, January, February and March) have the lowest values of mean precipitation (ca. 36 mm), and they coincide with the period of snow cover.

The Alta Badia valley, as part of the Dolomites in the Southern Alps, corresponds to a segment of the continental African margin that underwent to significant deformation from the Late Cretaceous to the Quaternary, firstly with European vergence and later, during the Cenozoic, with African vergence. The Dolomite region derived from the Tertiary shortening of the Mesozoic Tethys Ocean margin (Doglioni, 1987; Doglioni and Carminati, 2008) of subsidence and uplift. These processes controlled the development of Mesozoic carbonate platforms, surrounded by deep marine basins occasionally filled by volcanic, volcaniclastic and terrigenous sediments (Gianolla et al., 2009).

The main mountain groups, including Sella, Gardenaccia and Piz dles Conturines, are primarily composed of brittle Triassic dolomites (*Dolomia Cassiana* and *Dolomia Principale* formations) and ductile marls and silts (*Raibl Group*). The slopes beneath these mountains are formed by complex lithologies, such as Cretaceous volcanic breccias and pyroclastic rocks (*Fernazza Group and Caotico Eterogeneo*), Triassic pyroclastic sandstones and siltstones (*Wengen* Formation), and calcarenites, marls and silts (*S. Cassiano* Formation) (cf. Servizio Geologico d'Italia, 1977; Brandner et al., 2007).

The geomorphological setting of the area is characterized by high mountain peaks with deeply fractured vertical cliffs, separated by wide valleys with gentler and undulated slopes (Soldati, 2010; Marchetti et al., 2017). During the LGM the Alta Badia valley was covered by an extensive ice mass, coming from the north, which transitioned into local valley glaciers during the Lateglacial. In their topical book, Penck and Brückner (1909) firstly inferred that the primary feeding area of the LGM ice mass was from the Pusteria valley, located some 30 km northeast of the Alta Badia (Fig. 1). This hypothesis was resumed by Mutschlechner (1932, 1933) who implemented detailed geological maps also depicting widespread glacial deposits and erratic boulders, the transport of which was attributed to the LGM ice mass.

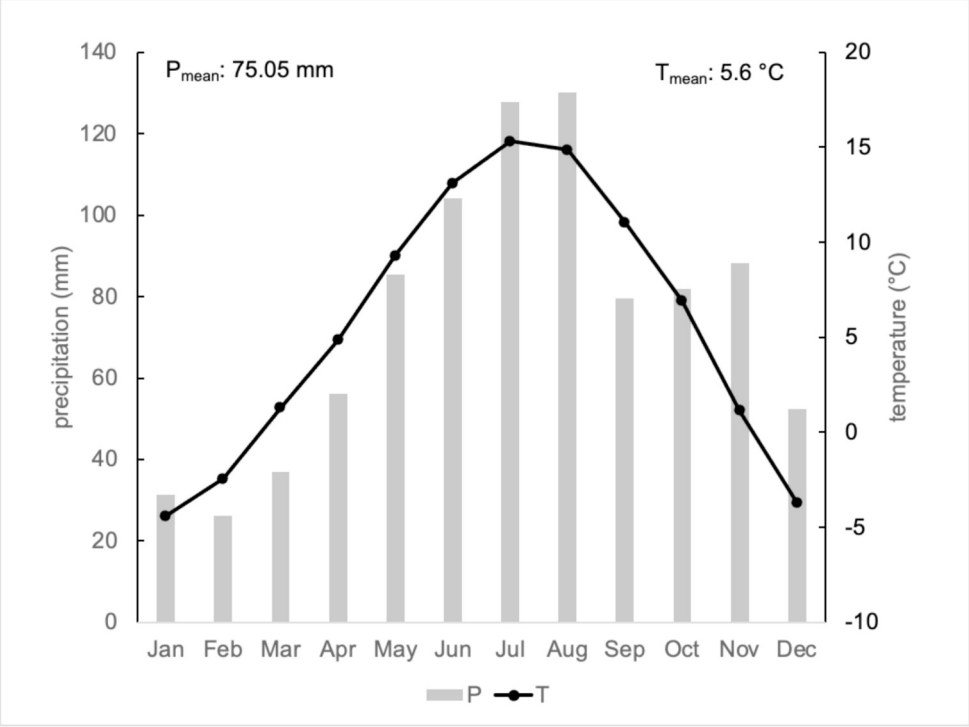

Fig. 2. Climograph derived from La Villa meteorological station data over the period 1987–2023 (station n. 61500BM, 46.583 N, 11.906 E, 1405 m a.s.l.). Data are available at the Autonomous Province of Bolzano - South Tyrol webpage (https://weather.provinz.bz.it/download-data.asp, last access 20 January 2025).

Landforms and processes in the valley are deeply controlled by lithological and tectonic features (Panizza, 1973; Corsini et al., 1999; Corsini et al., 2001; Soldati et al., 2004; Coratza et al., 2005; Borgatti et al., 2006; Soldati et al., 2006; Soldati and Borgatti, 2009; Panizza et al., 2011). Moreover, landscape evolution was influenced by the climatic changes occurred during the Quaternary. Glacial landforms are the oldest recognized in the valley and refer to both the LGM and the Lateglacial (Fig. 3; Panizza et al., 2011). More widespread and better preserved are the traces left by glaciers during the latter period including till deposits and moraine ridges whose position and elevation is fundamental for the reconstruction of glacial fluctuations (Ghinoi and Soldati, 2017).

The intense jointing of the dolomite massifs, glacial debuttressing as a consequence of the retreat of glaciers, as well as permafrost degradation, and the high relief energy have favoured the onset of rock falls and rock slides (Borgatti and Soldati, 2010). The water availability from rainfall and snow melt together with the poor geomechanical features of the terrains outcropping at the foothills of the dolomite massifs and within the valleys has favoured the occurrence of landslides mainly constituted by earth flows and slides, debris flows and composite debris cones (Corsini et al., 1999; Piacentini et al., 2012).

Over the past fifty years, the increased anthropic activity, i.e., tourism-related developments such as ski facilities, reshaped the original landscapes partially masking or even destroying landforms and deposits documenting past glacier fluctuations. In this context, a careful landscape analysis is particularly relevant to reconstruct the geomorphological evolution and glacial history.

3. Materials and methods

3.1. Geomorphological investigation and glacier reconstruction

Geomorphological investigations, including a thorough literature review, were carried out to retrieve geomorphological and glacial geological evidence contributing to the outline extension of the LGM icefield and of the glacier advances during the Lateglacial within the study area. This phase benefitted from the outputs of previous geomorphological studies available for the area, which provided information on the spatial distribution of glacial landforms (e.g., glacial cirques, trimlines and other erosion features, as well lateral and frontal moraines) and periglacial landforms (in the area mainly represented by rock glaciers).

Some information on the relative chronology of glacial features was also provided in literature (Castiglioni, 1940, 1964; Panizza et al., 2011; Ghinoi and Soldati, 2017). Preliminarily, based on previous geomorphological and geological maps (Mutschlechner, 1932, 1933; Castiglioni, 1964; Servizio Geologico d'Italia, 1977; Brandner et al., 2007; Panizza et al., 2011; Ghinoi and Soldati, 2017), the spatial information on glacial and periglacial landforms was manually collected in a GIS database using ArcMap 10.2 and Quantum Gis Desktop 3.10.2 (coordinate system UTM-WGS84 - Universal Transverse Mercator, zone 32, World Geodetic System 1984 datum). Geomorphological data derived from existing literature (Mutschlechner, 1932, 1933; Castiglioni, 1964; Servizio Geologico d'Italia, 1977; Brandner et al., 2007; Panizza et al., 2011; Ghinoi and Soldati, 2017), targeted field surveys, and remote sensed data analysis were digitized within a GIS environment.

Remote sensed data considered in this study includes: i) multiple aerial photograph arrays (1992/97, 2000, 2008, 2014) available on the on-line geoportal implemented by the Autonomous Province of Bolzano

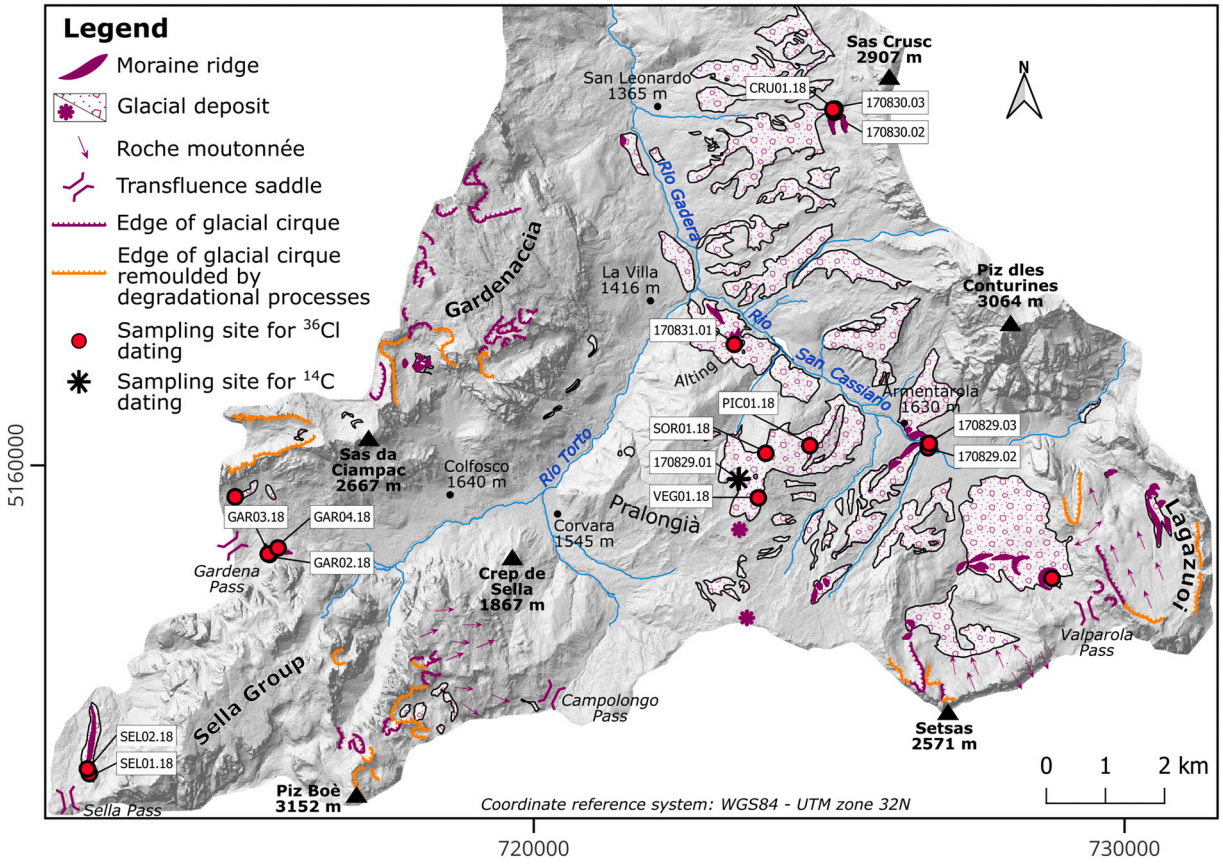

Fig. 3. Glacial landforms and deposits of the Alta Badia valley and Sella Pass area. Surface exposure dating and radiocarbon sampling sites are evidenced with red circles and asterisks, respectively. Glacial deposits not mappable at the scale of the map are indicated with the violet asterisk.

(2022), ii) LiDAR Digital Elevation Model (DEM) 2.5 × 2.5 m of spatial resolution courtesy of the Autonomous Province of Bolzano, iii) DEM 5 × 5 m of spatial resolution including the Belluno Province available at the geoportal of the Veneto Region (2020) and iv) Google Earth images.

Detailed geomorphological field surveys were crucial for ground-truthing data from literature and for providing a solid geomorphological framework for the reconstruction of LGM icefield and glacier outlines during the Lateglacial period.

The extension of the LGM icefield was reconstructed by identifying and mapping well preserved erosional trimlines (Fig. 4) located at the highest elevation. Paleoglaciers outlines and geometry (Fig. 5) were reconstructed on the basis of photointerpretation, and geomorphological and glacial geological field surveys. Glacial sediments distribution and limits, and well preserved erosional and depositional landforms provided the bases for reconstructing the position reached by glaciers during Lateglacial advance.

The Lateglacial glaciers' surface topography was reconstructed drawing vectorial contour lines of 50 m equidistance with a convex and a concave shape in the ablation and accumulation areas of glaciers, respectively, according to Porter (1975) and Porter and Orombelli (1982). Contour lines were interpolated to construct the digital terrain models (DTMs) of the Lateglacial glaciers. DTMs (5 × 5 m pixel size) were processed using ArcGIS 10.4 (ESRI software) by creating a Triangular Irregular Network (TIN) surface model from the reconstructed contour lines and using the conversion tool "TIN to raster".

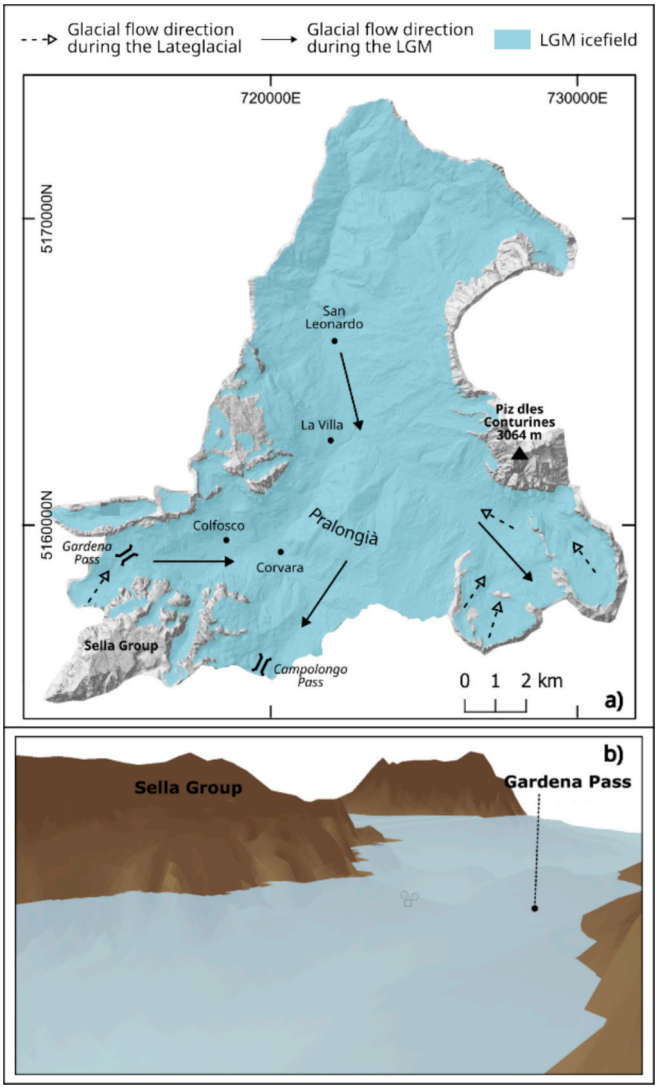

Fig. 4. Reconstruction of the LGM ice surface: (a) inferred extension and limits of the ice field covering the Alta Badia valley during the LGM; (b) glacier stand in correspondence of the Gardena Pass before 17.1 ka BP (glacier surface at 2300 m a.s.l.). Arrows indicate the ice flow direction during the LGM (from Marchetti et al., 2017 and references therein) and the Lateglacial (dashed arrows: Gschnitz stadial).

The Equilibrium Line Altitudes (ELAs) for each Lateglacial glaciers were calculated using both Accumulation Area ratio (AAR) and Area-Altitude Balance Ratio (AABR) methods, which are the most widely applied and consolidated method (Benn and Lehmkuhl, 2000; Kerschner et al., 2000; Porter, 2000; Benn and Ballantyne, 2005; Lukas, 2007; Stansell et al., 2007; Pellitero et al., 2016). We adopted an AAR of 0.67 ± 0.05 for valley glaciers and of 0.50 ± 0.05 for cirque glaciers (Porter, 1975); as regards the AABR, we applied two different Balance Ratio, considering recommendations for the Alpine region by Rea (2009) and by Oien et al. (2022), which indicate a value of 1.59 ± 0.6 and of 1.29, respectively. Hypsometry and ELA calculation were obtained with a free downloadable Python script running in ArcGIS Tool, the ELA Calculation Toolbox, which calculates the AAR-ELAs and AABR-ELAs automatically (Baroni et al., 2021).

The maximum thickness of the LGM ice mass was estimated by comparing the maximum elevation of the icefield with the lowest elevation at the valley bottom, based on LiDAR data of the present-day topography.

Lateglacial glaciers volume were calculated by comparing DTMs reconstructed for the Lateglacial phase and DTMs derived from LiDAR data, resampled at the same spatial resolution, using the Cut/fill tool in ArcGis.

3.2. Surface exposure dating

In situ cosmogenic ^{36}Cl surface exposure dating was used to infer the depositional ages of moraines within the Alta Badia valley. In order to perform cosmogenic ^{36}Cl dating, the sampling strategy focused on key selected sites considered as optimal for directly dating the LGM ice collapse and possible glacier advances during the Lateglacial.

The landscape in the study area has been heavily modified by intense anthropogenic activity and by gravity-induced processes; thus, extreme attention was paid in the selection of boulders for sampling. The key sites were selected not only because they retain the best-preserved glacial deposits, with clearly defined glacial geological and geomorphological features, but also because they display the best-preserved erratic boulders, clearly resting on the top of the crest of former frontal and lateral moraines and being unaffected by slope movements, potential burial and exhumation.

A total of 16 samples were collected from the top surfaces of these erratic boulders which were selected according to their position on the moraine crest, stability and size (Table 1). The detailed geomorphological field surveys on the moraines were crucial to select a reasonable number of boulders, suitable to successfully apply ^{36}Cl CRE. Location of sampling sites was taken by means of a hand-held GPS (Garmin) and elevation was derived from high resolution LIDAR data (Autonomous Province of Bolzano, 2022). In case of non-horizontal boulder tops, dip and inclination of the sampled surfaces also were measured through a magnetic compass. The topographic shielding factor was obtained by means of the "Point-based Shielding Model" GIS-tool devised by Li (2018).

3.2.1. Physical and chemical sample processing

The time of surface exposure can be calculated from measured concentration of cosmogenically-produced isotopes such as ^{36}Cl, ^{10}Be and ^{26}Al, in rocks or sediment. The time of exposure can be approximately considered as the time when the glacier started to retreat, that is, the minimum age of stabilization of the moraine deposit (cf. Ivy-Ochs and Briner, 2014).

In this study, ^{36}Cl was used because in the Alta Badia valley mainly

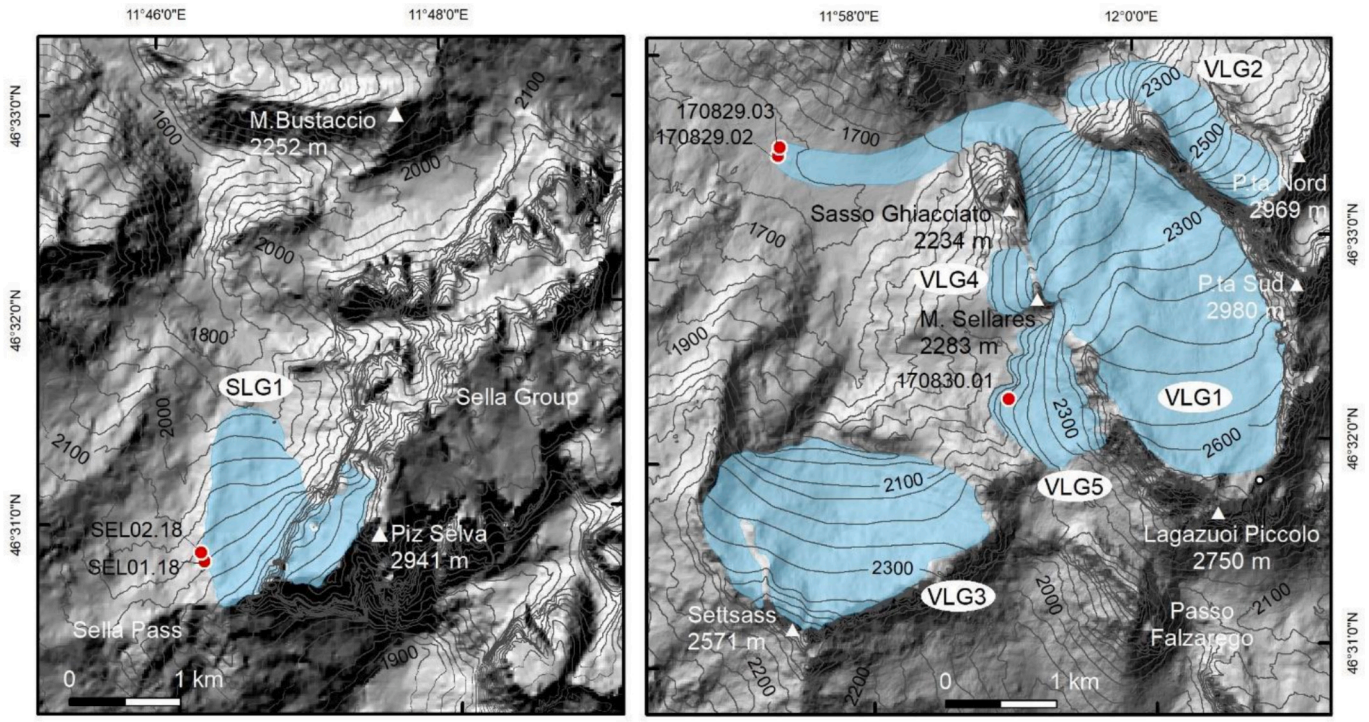

Fig. 5. Reconstruction of glacial bodies at Sella Pass (on the left) and at Valparola Pass (on the right) during the Lateglacial.

Table 1
Sample locations, attributes, and local corrections to production rates. The size of sampled erratic boulders is reported as length (L), width (W), and height (H).

Sampling site	Sample ID	Latitude WGS84	Longitude WGS84	Elevation (m a.s.l.)	Erratic boulder size L, H, W (cm)	Sample thickness	Shielding factor	Sampled unit
Armentarola	170829.02	46.56	11.96	1651	420, 170, 340	2.5	0.979	Moraine ridge
	170829.03	46.56	11.96	1652	410, 250, 210	2.5	0.983	Moraine ridge
Valparola	170830.01	46.54	11.98	2012	220, 180, 135	3.8	0.966	Ablation till
Sas Crusc	170830.02	46.61	11.94	2066	380, 350, 420	2.5	0.95	Moraine ridge
	170830.03	46.61	11.94	2049	600, 470, 390	3.5	0.939	Moraine ridge
	CRU01.18	46.61	11.94	2050	350, 120, 140	3.5	0.953	Moraine ridge
Alting	170831.01	46.57	11.92	1626	185, 175, 140	3	0.989	Moraine ridge
Gardena Pass	GAR01.18	46.55	11.80	2265	320, 240, 120	3	0.935	Ablation till
	GAR02.18	46.55	11.81	2235	380, 300, 120	2.5	0.931	Ablation till
	GAR03.18	46.55	11.81	2232	300, 270, 140	3	0.935	Ablation till
	GAR04.18	46.55	11.81	2196	300, 260, 140	3.5	0.927	Ablation till
Pralongià	SOR01.18	46.56	11.92	1973	230, 220, 90	2.5	0.990	Ablation till
	VEG01.18	46.55	11.92	1998	200, 120, 60	3	0.997	Ablation till
	PIC01.18	46.56	11.93	1852	3200, 1100, 1800	2.5	0.996	Ablation till
Sella Pass	SEL01.18	46.51	11.77	2192	700, 600, 300	2.5	0.959	Moraine ridge
	SEL02.18	46.51	11.77	2176	650, 500, 250	3	0.962	Moraine ridge

dolostone boulders can be found on moraines, and ^{36}Cl is abundantly produced in dolostone due to the high concentrations of the target element Ca in this lithotype. In fact, ^{36}Cl is produced through i) spallation of Ca, K, Ti and Fe (target elements), ii) slow-negative muon capture by K and Ca and iii) low-energy (thermal and epithermal) neutron capture by ^{35}Cl. Thus, the ^{36}Cl production in a rock strongly depends on its chemical composition and in particular on the concentration of the target elements and of other elements that modify the low-energy neutron flux (e.g., Li, B, Sm, Gd; cf. Schimmelpfennig et al., 2009).

The samples were physically and chemically prepared at CEREGE, France, following standard procedures proposed by Schlagenhauf et al. (2010) based on Stone et al. (1996). In particular, the physical preparation consisted in crushing and sieving the samples to retain the grain size fraction 250 μm–1000 μm for the extraction of the cosmogenic ^{36}Cl, while the grain size fractions <250 μm was used for chemical analysis of the bulk rock composition to calculate the low-energy neutron distribution in the dolostone samples. Before crushing, pictures of sample fragments selected to undergo physical and chemical preparation were taken and the thickness of each fragment was measured (Table 1).

Dry rock densities were determined in the laboratory based on the Archimedes principle on rock pieces (one representative for each sample) and they were found to vary between 2.7 and 2.8 g/cm^3. The chemical preparation was applied to 90–95 g of sample and to a blank solution used to track any contamination of Cl during the chemical preparation. The first step of chemical preparation consisted in the pretreatment of the samples aiming at eliminating atmospheric Cl, firstly with a washing with MQ water and secondly with HNO_3 (2 M), which dissolved about 10 % of the sample material. Then, after drying and weighing the remaining sample material (target fraction), an inhouse spike solution (carrier) of known $^{35}Cl/^{37}Cl$ ratio of 918 and containing ~2 mg of chlorine was added to the samples, allowing to determine the concentrations of both ^{36}Cl and total Cl in the sample simultaneously from one AMS measurement by the principle of isotope dilution (Ivy-Ochs et al., 2004; Desilets et al., 2006). After spiking, the samples were totally dissolved in HNO_3 (2 M). The solutions were filtered to remove any solid residues. Then, 1 ml aliquots of the sample solutions were collected to measure target element concentrations (Ca and K) in the target fraction, by inductive coupled plasma atomic emission spectrometry (ICP-AES) at CEREGE. After addition of $AgNO_3$, Cl precipitated from the sample and blank solutions in the form of AgCl. This precipitate was re-dissolved in NH_3(aq), then Cl was separated from S (including ^{36}S, an interfering isobar of ^{36}Cl) by the addition of $Ba(NO_3)_2$ causing the precipitation of $BaSO_4$, which was removed from the solutions by filtering. Finally, AgCl was re-precipitated by acidifying the solution with HNO_3, then recovered and dried for measurements of the $^{36}Cl/^{35}Cl$ and $^{35}Cl/^{37}Cl$ ratios at the French AMS national facility ASTER at CEREGE (Arnold et al., 2013).

3.2.2. Calculation of exposure ages

Calculation of exposure ages was performed using the Excel spreadsheet implemented by Schimmelpfennig et al. (2009). A ^{36}Cl production rate for spallation of Ca, referenced to sea level and high latitude (SLHL), of 42 ± 2 atoms ^{36}Cl (g Ca)$^{-1}$ yr^{-1} was used with the scaling method by Stone (2000) to convert production rates from SLHL to the sampled location. The chosen SLHL ^{36}Cl production rate for spallation of Ca was the one inferred by Braucher et al. (2011) by fitting modelled ^{36}Cl concentrations to ^{36}Cl measurements from a calcium carbonate core depth profile in south-eastern France, which is the nearest to the study area of the existing ^{36}Cl calibration sites. This value is also in agreement with the ^{36}Cl production rate for spallation of Ca calibrated by Schimmelpfennig et al. (2011) in Ca-rich feldspars from lava surface samples collected at Mount Etna volcano (Southern Italy). A production rate of epithermal neutrons from fast neutrons in atmosphere at land/atmosphere interface of 696 ± 185 n cm^{-2} a^{-1} was adopted (Marrero et al., 2016) and a high-energy neutron attenuation length of 160 g cm^{-2} was used. Spallation of Ca was revealed to be the main responsible for the production of ^{36}Cl in most of the samples (between 80 % and 30 %). Due to the relatively high natural chloride content measured in some of the samples (from <20 ppm to >200 ppm), the complex low-energy neutron production pathway contributed significantly to the total ^{36}Cl production (between 6 % and 64 %) causing an increase in the age estimation uncertainty (>10 %). A minor contribution in the total ^{36}Cl production was from negative muon capture reactions (between 4 % and 13 %).

In the lack of quantitative estimates for denudation of the dolostone formations in the Eastern Alps and considering that sampled boulders showed slight traces of erosion, the ages are discussed without any correction for denudation. These therefore correspond to minimum exposure ages. Snow shielding was not applied for boulders because they were supposed to stick out to the snow.

3.3. Radiocarbon dating

A targeted sampling site for radiocarbon dating (^{14}C) was identified along an artificial excavation wall at Pralongià (cf. Fig. 3), where Late Pleistocene glacial drift (lodgment till covered by ablation till) was deposited on top of the bedrock. We sampled bulk organic matter (ID 170829.02) from buried over-consolidated dark-brown soil preserved just above the bedrock and covered by lodgment till. The latter was constituted by heterometric massive diamicton matrix supported (silty-sand with clay). The clasts included dolostone gravel, angular to rounded striated cobbles and pebbles.

The sample was prepared and dated at CEDAD, the dating centre of the University of Salento and analysed using acceleration mass spectrometry (AMS). The provided conventional radiocarbon age was corrected for isotope fractionation by measuring $\delta^{13}C$ with AMS and for background. The age was calibrated in calendar years using the software CALIB Ver. 8.2 (cf. Reimer et al., 2020). Calibrated age is reported with two standard deviations.

4. Results

4.1. Glacial geological and geomorphological evidence of LGM glacial retreat

The reconstruction of the LGM ice surface showed that the icefield covering the Alta Badia and surrounding valleys reached a maximum elevation of ca. 2400 m a.s.l. (Fig. 4). Local glaciers flowing from the Gardenaccia and Sella groups, as well as from the Setsas and Lagazuoi mounts, joined and flowed into the icefield.

The LGM icefield covering the Alta Badia valley extended for some 160 km^2 reaching a maximum thickness of approximately 1300 m. Below the upper trimline of the LGM, we have identified geomorphological and glacial geological evidence of glacial mass stagnation and collapse. Well defined glacial deposits and moraines deposited ca. 100 m below the uppermost trimline at Gardena Pass document the stationing of the glacial surface during the early stages of glacier retreat.

Other evidence of the early phases of glacial collapse after the LGM were identified at Pralongià and Sella Pass. In the latter locality, as evidenced at Gardena Pass, glacial deposits and moraines were deposited below the LGM trimline. On the Pralongià Plateau, which represents a summit area covered during the LGM, we identified melt out tills carrying erratic boulders and resting on lodgment till that, in turn, covered the local bedrock. Meltout till and erratic boulders were deposited during the early phases of glacial collapse after the LGM and were not associated with obvious phases of glacial readvance.

In the study area, numerous patches of glacial deposits outcrop both inside the valleys and on the intervening reliefs that, at many sites, define well evident moraine ridges. We recognized that some ridges are clearly associated with glacial readvances, while in other cases they document recessional moraines. Steep moraines defining glacial advances were recognized in the Sella Pass area, and upstream of the Armentarola locality in Valparola (Fig. 3). Additional evidence of moraines located at high elevation were investigated at Sas Crusc along the western slope of the Conturines Group, in the northern portion of the study area.

Based on these new data and interpretation, we reconstructed the limits of paleoglaciers related to glacial advances to define their areal extent and ELA using both AAR and AABR method (Figs. 5 and 6; Tables 2 and 3). Glaciological data for the reconstructed paleoglaciers are reported in Table 2. Areal extension of the paleoglaciers range from 0.2 km^2 to 5.6 km^2 while ELAs range from 2120 m +5/−10 and 2320 m +25/−20 m applying the AAR method. When applying the AABR method, the ELAs range from 2110 +10/−5 m and 2360 +50/−35, and 2120 and 2185 considering the balance ratios suggested by Rea (2009) and Oien et al. (2022) respectively (Fig. 6; Table 3).

The agreement among the different ELA methods is very good, with the only exception of SLG1 glacier. The difference in ELA values can be attributed to the peculiar morphology of the feeding basin, which is distributed over two sectors separated by an altitudinal step that is not computed with the AAR method, beeing strictly linked to local

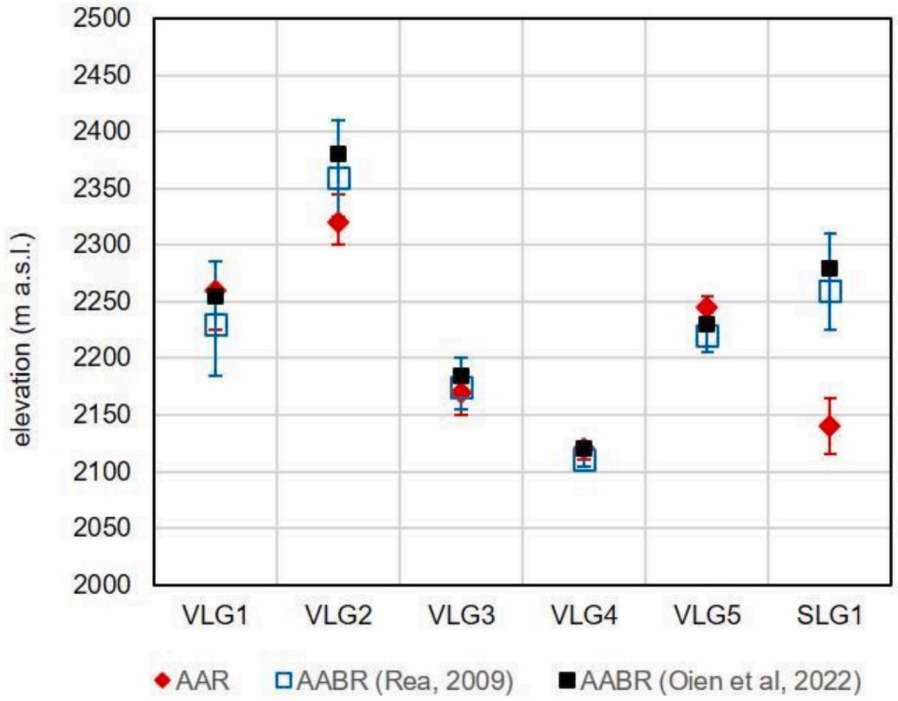

Fig. 6. Distribution of reconstructed Equilibrium Line Altitude (ELA). For the AABR, the elevation values were calculated according to both Rea (2009) and a more recent study by Oien et al. (2022).

Table 2
Glacier ID, midpoint coordinates, and morphometric parameters of the reconstructed glaciers in the Alta Badia area. The tongue of the reconstructed VLG1 glacier infilled a valley sector currently occupied by extensive scree cones; therefore the volume resulting from the difference between the reconstructed paleosurface and present-day topography is underestimated (*).

Glacier ID	Latitude N	Longitude E	Area (km^2)	Volume (km^3)	Length max (m)	Width max (m)	Elevation (m)		Mean aspect	Mean slope (°)
							Min	Max		
SLG1	46.517	11.778	1.68	0.058	1811	1122	1903	2781	NNW	26
VLG1	46.547	11.998	5.62	0.409*	6182	1701	1183	2723	N	14
VLG2	46.559	12.006	0.95	0.036	2374	503	1817	2841	NW	23
VLG3	46.528	11.963	3.26	0.273	1731	2585	1750	2533	N	24
VLG4	46.547	11.985	0.2	0.009	409	599	2013	2234	W	28
VLG5	46.538	11.989	0.91	0.074	893	1290	2000	2487	W	29

Table 3
Reconstructed Equilibrium Line Altitude (ELA) using both the AAR and AABR methods. For the AABR method, two Balance Ratio values were applied: 1.59 (*) and 1.29 (**) according to Rea (2009) and Oien et al. (2022), respectively.

Glacier ID	ELA – AAR				ELA-AABR			
	AAR	(m a.s.l.)	AAR + 0.05 (m a.s.l.)	AAR −0.05 (m a.s.l.)	AABR* 1.59 (m a.s.l.)	1.59 + 0.6 (m a.s.l.)	1.59 − 0.6 (m a.s.l.)	AABR** 1.29 (m a.s.l.)
VLG1	0.67	2260	2225	2285	2230	2185	2285	2255
VLG2	0.67	2320	2300	2345	2360	2325	2410	2380
VLG3	0.67	2170	2150	2185	2175	2155	2200	2185
VLG4	0.50	2120	2110	2125	2110	2105	2120	2120
VLG5	0.50	2245	2230	2255	2220	2205	2240	2230
SLG1	0.67	2140	2115	2165	2260	2225	2310	2280

topographic conditions (Osmaston, 2005; Porter, 1975; Rea, 2009).

4.2. Cosmogenic and radiocarbon dates

Detailed geomorphological and glacial geological field surveys allowed us to select seven key sites to chronologically constrain paleoglacier evolution in the study area (Figs. 3 and 7). In Table 4 the ^{36}Cl ages are reported with their overall uncertainty, which considers both the analytical error and the production rate error. This uncertainty must be considered when comparing ages at regional scale. Additionally, in Table 4, for the sake of internal comparison between all ^{36}Cl ages, the latter are presented with the analytical errors only, thus excluding from the estimate the error contribution due to the production rates. Sampling sites are described here below moving clockwise from the Sella Pass at the SW edge of the study area.

a) At Sella Pass, we sampled two dolostone boulders (at 2176 and 2192 m a.s.l.) on top of a lateral moraine stretching northward for approximately 800 m (SEL01.18 and SEL02.18), which dated to 15.8 ± 3.4 and 15.4 ± 2.8 ka BP, respectively.

Fig. 7. Location of some of the dated boulders' sampling sites: a), c) Gardena Pass (southern side); b) Valparola; d) Alting; e) Pralongià.

b) At Gardena Pass, we collected four samples of dolostone erratic boulders at elevations ranging between ca. 2190 and 2265 m a.s.l. The boulders rest on top of ablation till mainly constituted by dolostone cobbles and boulders, widespread all along the slope and constituting a ca. 5 m thick blanket on the bedrock. One sample was collected from the northern part of the Gardena Pass (GAR01.18) at 2265 m, in correspondence of a glacial deposit ascribed by Brandner et al. (2007) and Panizza et al. (2011) to the LGM on the basis of its relatively high position. This sample was dated at 9.9 ± 3.2 ka BP. The other samples (GAR02.18; GAR03.18; GAR04.18) were collected from erratic boulders located on a moraine elongated on the north-facing slopes of the Gardena Pass scattered from 2196 m a.s.l. to 2135 m a.s.l., which furnished ^{36}Cl ages spanning from 13.4 ± 1.4 and 17.1 ± 2.5 ka BP (Figs. 3, and 8; Table 4).

c) The Sas Crusc sampling site lies in the northern portion of the study area along the western slope of the Conturines Group. A set of two moraines located at about 2050 m a.s.l. at the base of Sas Crusc rock cliff was investigated. We selected the lowermost ridge for sampling three dolostone boulders located on top of the moraine. The samples (170830.02, 170830.03; CRU01.18) supplied ^{36}Cl ages spanning from 6.3 ± 0.6 and 9.8 ± 1.1 ka BP (Figs. 3 and 8; Table 4).

d) The Alting sampling site is located in the central sector of the study area at ca. 1600 m a.s.l., near the eponymous ski run. A discontinuous lateral moraine system elongated in a north to north-western direction was identified and mapped. A dolostone boulder suitable to be dated was selected on top of the uppermost portion of the ridge and dated at 14.4 ± 1.3 ka BP (170831.01; Figs. 3, 7, and 8; Table 4).

e) On the Pralongià isolated plateau, located in the central sector of the study area, we sampled three erratic boulders between 1852 and 1998 m a.s.l. (SOR01.18; VEG01.18; PIC01.18), which supplied ^{36}Cl ages ranging from 13.6 ± 2.4 to 18.0 ka BP (Figs. 3 and 8; Table 4). In addition, a sample of bulk organic sediment (170829.01) collected

Table 4
^{36}Cl exposure ages of the collected samples. Ages are reported with their uncertainty which takes into account both analytical and production rate errors (1-sigma). The analytical (inner) uncertainty is reported in brackets.

Sampling site	Sample ID	Age (ka BP)	Elevation (m a.s.l.)
Armentarola	170829.02	13.3 ± 1.4 (1.0)	1651
	170829.03	14.3 ± 2.1 (1.3)	1652
Valparola	170830.01	14.4 ± 2.8 (1.8)	2012
Sas Crusc	CRU01.18	9.8 ± 1.1 (0.9)	2050
	170830.02	6.3 ± 0.6 (0.5)	2066
	170830.03	9.5 ± 1.0 (0.7)	2049
Alting	170831.01	14.4 ± 1.3 (1.0)	1626
Gardena Pass	GAR01.18	9.9 ± 3.2 (2.8)	2265
	GAR02.18	17.1 ± 2.5 (2.0)	2235
	GAR03.18	13.4 ± 1.4 (1.2)	2232
	GAR04.18	15.9 ± 2.2 (1.8)	2196
Pralongià	SOR01.18	14.8 ± 2.6 (2.0)	1973
	VEG01.18	13.6 ± 2.4 (1.8)	1998
	PIC01.18	18.0 ± 2.8 (2.2)	1852
Sella Pass	SEL01.18	15.8 ± 3.4 (2.7)	2192
	SEL02.18	15.4 ± 2.8 (2.1)	2176

near La Brancia refuge at 1899 m a.s.l., on top of the weathered marls bedrock (S. Cassiano Formation, Carnian in age) covered by a lodgement till of LGM supplied an average ^{14}C age of 39,498 ± 493 cal. a BP (LTL-19640A; Table 5).

f) The Armentarola sampling site is located in the south-eastern sector of the study area within the valley bottom at ca. 1600 m a.s.l. where several moraine ridges and widespread glacial deposits were studied and mapped. These deposits were firstly recognized by Mutschlechner (1933) and Castiglioni (1964) and Panizza et al. (2011) ascribed them to the Lateglacial period. In a topmost position of a well-preserved moraine, we collected two samples from dolostone boulders for ^{36}Cl dating. The samples (170829.02; 170829.03) supplied two ages of 13.3 ± 1.4 and 14.3 ± 2.1 ka BP (Figs. 3 and 8; Table 4).

g) The Valparola sampling site is located at about 2000 m a.s.l. in the south-eastern sector of the study area. Several frontal moraine ridges arranged in sequence were identified and mapped; they witness different glacial phases, one of which was interpreted as evidence of a glacial advance. We collected one sample (170830.01) on top of this moraine from a dolostone boulder, which furnished an age of 14.4 ± 2.8 ka BP.

Radiocarbon dating of the sample collected from exposed deposits on the Pralongià Plateau revealed an uncalibrated ^{14}C age of 34,285 ± 230 a BP and a median calibrated age of about 39,498 ± 493 cal. a BP (Table 5).

5. Discussion and interpretation

The reconstruction of the LGM ice surface depicts an icefield occupying the Alta Badia and surrounding valleys, which extended about 160 km^2 and covered the main saddles to the maximum elevation of about 2400 m a.s.l. at Sella and Gardena passes (Fig. 4). Local glaciers nesting in the Gardenaccia and Sella groups, as well as from the Setsas and Lagazuoi mounts, contributed to the feeding the main icefield. At the valley bottom, the maximum estimated thickness of the icefield was about 1300 m. The exposure ages of the dated moraine boulders range within a wide period, from 18 ± 2.2 to 6 ka BP ± 0.5 ka BP (Fig. 8; Table 4). The ages of 12 samples out of 16 are from the Late Pleistocene, while only four samples revealed a Holocene exposure time. The oldest dates refer to two samples, one collected from the erratic mass located on the eastern slope of the Pralongià Plateau (18.0 ± 2.8 ka BP) and the other one at the southern side of the Gardena Pass (17.1 ± 2.5 ka BP). However, ten samples revealed ^{36}Cl ages between 12 and 16 ka BP, i.e., at the sampling sites of Armentarola, Valparola, Alting, Gardena and Sella passes, and Pralongià Plateau (Table 4). Landscape analysis and SED suggest that the early stage of post-LGM glacier retreat predates 17 ka BP at Gardena Pass where a well-defined moraine ridge witnesses a stillstand phase of the glacial body at an elevation of about 2200 m. The Pralongià Plateau was ice covered until 18 ka BP as documented by dates obtained from erratic boulders on top of ablation till resting on LGM lodgement till postdating organic sediment dated to 39.5 cal. ka BP (at ca. 1850 m, Table 5).

Our findings underline that the icefield gradually collapsed after the LGM leaving recessional moraines and patches of glacial ablation till at different elevation. Furthermore, residual glaciers from the original ice mass developed in the main valleys adjusting their shape to local morpho-topographic conditions as a consequence of glacier surface lowering. Post-LGM glaciers collapse is documented in many sites in the Alpine chain and its margin (Kelly et al., 2004; Scapozza et al., 2014; Ivy-Ochs, 2015; Reitner et al., 2016; Wirsig et al., 2016). The onset of ice surface lowering in the internal portion of the chain was almost synchronous to the downwasting of valley glaciers and piedmont lobes at both the northern and southern foreland margins (at ca. 19–18 ka BP; Wirsig et al., 2016).

Remnants of LGM glaciers were abandoned within the study area as well documented in other internal sector of the Alps (e.g., Mont Blanc area, Zillertal Alps, Lienz area, Central and Western Swiss Alps; Kelly et al., 2004; Ivy-Ochs, 2015; Reitner et al., 2016; Wirsig et al., 2016). The residual ice masses and local morpho-topographic constraints preserved thick ice bodies within the main valley depressions and led to thin glacial cover on intervening ridges. During this phase glacial fluxes were in Alta Badia opposite with respect to the LGM ice flow direction, which is to our knowledge an uncommon, if not unique, situation so far described in the Alps. In fact, the morphology of Alpine valley systems generally controlled ice flow direction from the high interior Alps toward the foreland areas, even where glacial erosion resulted in overdeepened basins (Preusser et al., 2011; Reitner et al., 2016; Wirsig et al., 2016; Gegg and Preusser, 2023). Stationing of glacial masses in the Alta Badia valley is well documented at Pedraces (Rio Gardena) and Alting (Fig. 3) by well evident frontal and lateral moraines (Castiglioni, 1964; Panizza et al., 2011), showing glacier flow direction from SE to NW, opposite to LGM ice flux direction. Castiglioni (1964) ascribed the Pedraces moraine to the early Lateglacial Sciliar phase. We did not find erratics suitable for sampling on these moraines but we agree with Castiglioni's interpretation and suggest to attribute these moraines to the early stage of glacier collapse after the LGM. On the other hand, our data suggest that residual ice masses persisted on the Pralongià Plateau until about 14 ka BP (Figs. 3 and 8; Table 4).

We recognized and chronologically constrained Lateglacial readvances in the Sella Pass area and Valparola (to the SE of Armentarola). The Lateglacial ice body reconstructed in the Sella Pass area (SLG 1 glacier in Fig. 5) was bordered by a well evident lateral moraine, which can be attributed to the Gschnitz Phase based on two minimum ^{36}Cl ages (15.8 and 15.4 ka BP; Figs. 2, 4 and 7; Table 4). The reconstructed glacier body descended toward NNW from a glacier cirque sculpted on the Piz Selva and extended 1.68 km^2 (Table 2). The reconstructed ELA (Fig. 6; Table 3) was located at 2140 m ± 25 (AAR method) and 2260 +50/−35 m (AABR method considering a balance ratio of 1.59) and 2280 (AABR method considering a balance ratio of 1.29).

The Valparola Lateglacial glaciers (VLG1 to 5; Fig. 5) had different shape and size; their morphometric and glaciological features are summarized in Table 2. The reconstructed ELAs range from 2120 m +5/−10 and 2320 m +25/−20 m applying the AAR method while 2110 +10/−5 m and 2360 +50/−35 m, and 2120 m and 2380 applying the AABR method according to Rea (2009) and Oien et al. (2022), respectively (Fig. 6; Table 3). Based on three surface exposure ages of ^{36}Cl ranging between 13.3 ka BP and 14.4 ka BP, which strictly refer to a glacier advance postdating the Gschnitz phase and predating the Egesen Lateglacial advance, we tentatively suggest relating the reconstructed glaciers in Valparola to the traditional Daun Lateglacial phase. It should be

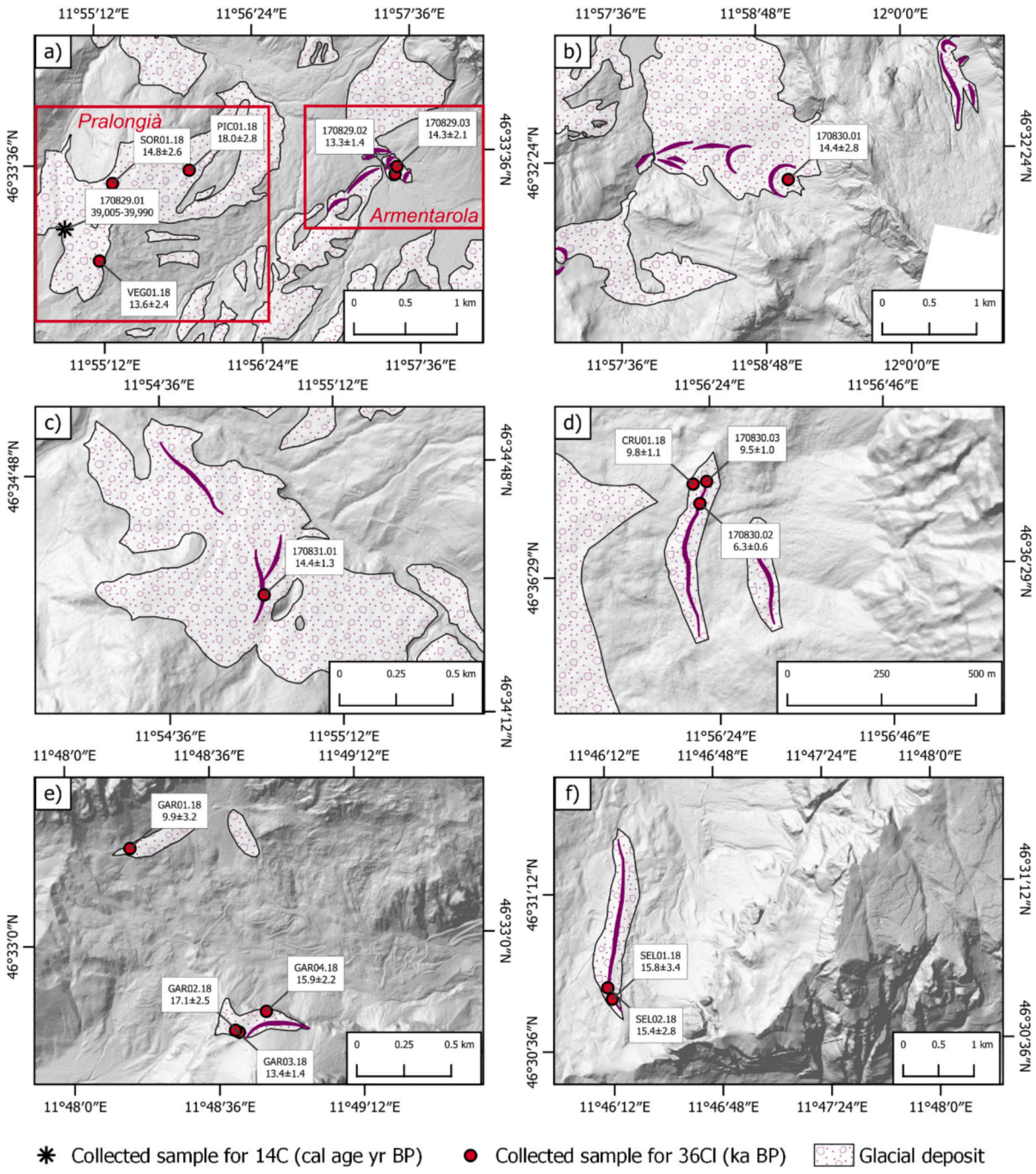

Fig. 8. Detail of the sampled key sites: a) Pralongià and Armentarola; b) Valparola; c) Alting; d) Sas Crusc; e) Gardena Pass; f) Sella Pass.

Table 5
^{14}C dating results for the sample 170829.01 collected from a subsurface deposit exposed on the Pralongià Plateau.

Sample ID	Lab code	^{14}C age a BP	St dev	δ^{13}C (‰)	Cal. age a BP (2σ)
170829.01	LTL-19640A	34,285	230	−31.4 ± 0.3	39,005–39,990

noted that the reconstructed ELAs both with AAR and AABR methods show a significant range of variability, which can however be explained considering the different shape and size of the paleoglaciers, as well as the morpho-topographic setting of the bedrock underlying the reconstructed glaciers.

After the second Lateglacial advance phase that we recognized, the Alta Badia area was almost completely deglaciated with only small glacier remnants being confined in the most elevated and protected location. The most recent advance in the area is recorded by the moraine at the toe of Sas Crusc rock cliff that we dated at 9.5–9.8 ka BP (Fig. 8). This moraine was deposited by a small glacier developed on the western slope of the Sass Crusc and covers glacial deposits associated with the initial phase of withdrawal after LGM and slope debris. Considering that the dates we obtained supply a minimum age for this moraine, we can tentatively associate this glacier advance to the Egesen Lateglacial phase. On the other hand, the date of 6.3 ka BP from a boulder resting on the ridge would suggest that this moraine could have been reached after its deposition by blocks detached from the overhanging rock cliff. The occurrence of falling blocks on the moraine would not exclude an older

age for this deposit as suggested by Panizza et al. (2011), who attributed the ridge to the LGM. However, we did not find evidence of an extensive landslide deposit constituted by huge blocks as reported by Brandner et al. (2007).

The scarcity of suitable boulders for dating in some of the investigated sites – including Valparola, Alting and Gardena Pass sampling sites – limits the ability to rely on populations of ages to refine the glacial chronology. This limitation is partly due to the highly dynamic landscape evolution, significantly influenced by slope instability processes. These processes, active since at least 10,700 years BP (cf. Soldati et al., 2006; Borgatti and Soldati, 2010), have led to the reworking and alteration of glacial deposits, posing challenges in identifying well-preserved geomorphic units of glacial origin and in sampling stable boulders that were not remobilized by slope instability processes, ensuring their suitability for surface exposure dating.

6. Conclusions

This study showcases a detailed reconstruction of the LGM and subsequent glacial history in the Alta Badia valley. Our findings provide meaningful insights into the timing and mode of glacial retreat in the valley and surroundings, laying the ground for future studies on climate fluctuations during deglaciation in this region. Based on geomorphological evidence and ^{36}Cl dating, applied here for the first time in the Eastern Dolomites, we provide new insights into the glacial retreat patterns of the region, contributing to the understanding of post-LGM glacial evolution. The analysis of the maximum elevation of the trimlines revealed that the LGM icefield reached the maximum elevations of around 2400 m a.s.l. at the main mountain passes and extended approximately 160 km^2 within the Alta Badia valley. After the LGM, the icefield collapse led to the formation of moraines, glacial ablation till and residual glaciers adjusting to local topographic conditions. Dating evidence indicates that the early stages of post-LGM glacier retreat occurred before 17 ka BP. However, extensive sectors of the investigated area remained ice-covered until about 18 ka BP. The peculiarity of the inversion of glacial flow in remnant glaciers after LGM was driven by the local morphology of the study area, which, at our knowledge, is here firstly documented and dated within the Alpine chain.

Notably, Gschnitz (15.8–15.4 ka BP) and Daun (ca. 14.4–13.3 ka BP) Lateglacial phases were identified thanks to the presence of evident lateral and frontal moraines in the investigated key sites, which were crucial for the reconstruction of glacier surfaces and ELA, and for dating glacial deposits through ^{36}Cl surface exposure ages. In contrast, the most recent Lateglacial advance (Egesen) is less clearly definable. A moraine dated to 9.8–9.5 ka BP may represent a late-stage advance. However, the landscape of the investigated valley is highly dynamic, and slope deposits may have covered the Egesen moraines.

CRediT authorship contribution statement

Carlo Baroni: Writing – review & editing, Writing – original draft, Validation, Supervision, Resources, Project administration, Methodology, Investigation, Funding acquisition, Conceptualization. **Maria Cristina Salvatore:** Writing – review & editing, Writing – original draft, Visualization, Validation, Supervision, Resources, Methodology, Investigation, Formal analysis, Data curation, Conceptualization. **Vittoria Vandelli:** Writing – review & editing, Writing – original draft, Visualization, Validation, Resources, Methodology, Investigation, Formal analysis, Data curation, Conceptualization. **Mauro Marchetti:** Resources, Investigation, Conceptualization. **Mauro Soldati:** Writing – review & editing, Writing – original draft, Validation, Supervision, Resources, Project administration, Methodology, Investigation, Funding acquisition, Conceptualization.

Declaration of competing interest

The authors declare that they have no known competing financial interests or personal relationships that could have appeared to influence the work reported in this paper.

Acknowledgments

The research was carried out in the frame of the following projects: (i) “Monitoring of the geological and geomorphological attributes of the Dolomites World Heritage Site” funded by UNESCO Dolomites Foundation – Scientific responsible: Mauro Soldati; (ii) University of Pisa research grants (Carlo Baroni, Maria Cristina Salvatore, Ateneo 2018–2020); (iii) SPaceItUp, funded by the Italian Space Agency, ASI, and the Ministry of University and Research, MUR, under contract n. 2024-5-E.0 - CUP n. I53D24000060005. We wish to thank the two anonymous reviewers for their constructive comments, which helped us to improve the manuscript.

Data availability

The data that support the findings of this study are available from the corresponding author upon reasonable request.

References

Arnold, M., Aumaître, G., Bourlès, D.L., Keddadouche, K., Braucher, R., Finkel, R.C., Nottoli, E., Benedetti, L., Merchel, S., 2013. The French accelerator mass spectrometry facility ASTER after 4 years: status and recent developments on 36Cl and 129I. Nucl. Instrum. Methods Phys. Res., Sect. B 294, 24–28. https://doi.org/10.1016/j.nimb.2012.01.049.

Autonomous Province of Bolzano, 2022. GeoCatalogo - on-line geoportal of the Autonomous Province of Bolzano [WWW Document]. URL. http://geokatalog.buergernetz.bz.it/geokatalog/#! (accessed 8.22.24).

Baroni, C., Gennaro, S., Salvatore, M.C., Ivy-Ochs, S., Christl, M., Cerrato, R., Orombelli, G., 2021. Last Lateglacial glacier advance in the Gran Paradiso Group reveals relatively drier climatic conditions established in the Western Alps since at least the Younger Dryas. Quaternary Science Reviews 255, 106815. https://doi.org/10.1016/j.quascirev.2021.106815.

Benn, D.I., Ballantyne, C.K., 2005. Palaeoclimatic reconstruction from Loch Lomond Readvance glaciers in the West Drumochter Hills, Scotland. Journal of Quaternary Science 20, 577–592. https://doi.org/10.1002/jqs.925.

Benn, D.I., Lehmkuhl, F., 2000. Mass balance and equilibrium-line altitudes of glaciers in high-mountain environments. Quat. Int. 65–66, 15–29. https://doi.org/10.1016/S1040-6182(99)00034-8.

Bernsteiner, H., Götz, J., Salcher, B.C., Lang, A., 2021. From deglaciation to postglacial filling: post-LGM evolution of an isolated glacier system at the northern fringe of the Eastern Alps (Austria). Geogr. Ann. Ser. A 103, 305–322. https://doi.org/10.1080/04353676.2021.1933958.

Borgatti, L., Soldati, M., 2010. Landslides as a geomorphological proxy for climate change: a record from the Dolomites (northern Italy). Geomorphology 120, 56–64. https://doi.org/10.1016/j.geomorph.2009.09.015.

Borgatti, L., Ravazzi, C., Donegana, M., Corsini, A., Marchetti, M., Soldati, M., 2006. A lacustrine record of early Holocene watershed events and vegetation history, Corvara in Badia, Dolomites (Italy). Journal of Quaternary Science 22, 173–189. https://doi.org/10.1002/jqs.1039.

Brandner, R., Keim, L., Gruber, A., Gruber, J., 2007. Geologische Karte der Westlichen Dolomiten-Carta Geologica delle Dolomiti Occidentali 1: 25.000. Autonome Provinz Bozen-Südtirol-Provincia Autonoma di Bolzano-Alto Adige. Amt für Geologie & Baustoffprüfung-Ufficio Geologia e Prove Materiali, Kardaun/Cardano (BZ).

Braucher, R., Merchel, S., Borgomano, J., Bourlès, D.L., 2011. Production of cosmogenic radionuclides at great depth: a multi element approach. Earth Planet. Sci. Lett. 309, 1–9. https://doi.org/10.1016/j.epsl.2011.06.036.

Castiglioni, B., 1940. L'Italia nell'età quaternaria. Carta delle Alpi nel Glaciale (scala 1: 200 000). Consociazione Turistica Italiana, Milano.

Castiglioni, G.B., 1964. Sul morenico stadiale delle Dolomiti. Memorie dell'Istituto di Geologia e di Mineralogia dell'Università di Padova 24, 1–16.

Clark, P.U., Dyke, A.S., Shakun, J.D., Carlson, A.E., Clark, J., Wohlfarth, B., Mitrovica, J.X., Hostetler, S.W., McCabe, A.M., 2009. The last glacial maximum. Science 325, 710–714. https://doi.org/10.1126/science.1172873.

Clark, P.U., Shakun, J.D., Baker, P.A., Bartlein, P.J., Brewer, S., Brook, E., Carlson, A.E., Cheng, H., Kaufman, D.S., Liu, Z., Marchitto, T.M., Mix, A.C., Morrill, C., Otto-Bliesner, B.L., Pahnke, K., Russell, J.M., Whitlock, C., Adkins, J.F., Blois, J.L., Clark, J., Colman, S.M., Curry, W.B., Flower, B.P., He, F., Johnson, T.C., Lynch-Stieglitz, J., Markgraf, V., McManus, J., Mitrovica, J.X., Moreno, P.I., Williams, J.W., 2012. Global climate evolution during the last deglaciation. Proc. Natl. Acad. Sci. 109, E1134–E1142. https://doi.org/10.1073/pnas.1116619109.

Coratza, P., Marchetti, M., Soldati, M., 2005. Geomorfologia ed instabilità dei versanti del Gruppo del Sassolungo (Dolomiti occidentali). Geogr. Fis. Din. Quat. Suppl. VII, 105–113.
Corsini, A., Pasuto, A., Soldati, M., 1999. Geomorphological investigation and management of the Corvara landslide (Dolomites, Italy). Japanese Geomorphological Union Transactions 20, 169–186.
Corsini, A., Marchetti, M., Soldati, M., 2001. Holocene slope dynamics in the area of Corvara in Badia (Dolomites, Italy): chronology and paleoclimatic significance of some landslides. Geogr. Fis. Din. Quat. 24, 127–139.
Desilets, D., Zreda, M., Almasi, P.F., Elmore, D., 2006. Determination of cosmogenic 36Cl in rocks by isotope dilution: innovations, validation and error propagation. Chem. Geol. 233, 185–195. https://doi.org/10.1016/j.chemgeo.2006.03.001.
Doglioni, C., 1987. Tectonics of the Dolomites (southern alps, northern Italy). J. Struct. Geol. 9, 181–193. https://doi.org/10.1016/0191-8141(87)90024-1.
Doglioni, C., Carminati, E.A.M., 2008. Structural styles and Dolomites field trip. Memorie Descrittive della Carta Geologica d'Italia 82, 1–293.
Federici, P.R., Granger, D.E., Pappalardo, M., Ribolini, A., Spagnolo, M., Cyr, A.J., 2008. Exposure age dating and Equilibrium Line Altitude reconstruction of an Egesen moraine in the Maritime Alps, Italy. Boreas 37, 245–253. https://doi.org/10.1111/j.1502-3885.2007.00018.x.
Gegg, L., Preusser, F., 2023. Comparison of overdeepened structures in formerly glaciated areas of the northern Alpine foreland and northern central Europe. Quaternary Science Journal 72 (23–36), 2023. https://doi.org/10.5194/egqsj-72-23-2023.
Ghinoi, A., Soldati, M., 2017. Reappraisal of Lateglacial stadials in the Eastern Alps: the case study of Valparola (Eastern Dolomites, Italy). Alpine and Mediterranean Quaternary 30, 51–67.
Gianolla, P., Andreetta, R., Furin, S., Furlanis, S., Riva, A., 2009. Annex 2 - geology. In: Nomination of the Dolomites for Inscription on the World Natural Heritage List UNESCO. Artimedia, Trento, Italy, pp. 1–77.
Ivy-Ochs, S., 2015. Glacier variations in the European Alps at the end of the last glaciation. Cuadernos de Investigacion Geografica 41, 295–315. https://doi.org/10.18172/cig.2750.
Ivy-Ochs, S., Briner, J.P., 2014. Dating disappearing ice with cosmogenic nuclides. Elements 10, 351–356. https://doi.org/10.2113/gselements.10.5.351.
Ivy-Ochs, S., Synal, H.-A., Roth, C., Schaller, M., 2004. Initial results from isotope dilution for Cl and 36Cl measurements at the PSI/ETH Zurich AMS facility. Nucl. Instrum. Methods Phys. Res., Sect. B 223–224, 623–627. https://doi.org/10.1016/j.nimb.2004.04.115.
Ivy-Ochs, S., Kerschner, H., Kubik, P.W., Schlüchter, C., 2006. Glacier response in the European Alps to Heinrich Event 1 cooling: the Gschnitz stadial. J. Quat. Sci. 21, 115–130. https://doi.org/10.1002/jqs.955.
Ivy-Ochs, S., Kerschner, H., Reuther, A., Preusser, F., Heine, K., Maisch, M., Kubik, P.W., Schlüchter, C., 2008. Chronology of the last glacial cycle in the European Alps. Journal of Quaternary Science 23, 559–573. https://doi.org/10.1002/jqs.1202.
Ivy-Ochs, S., Monegato, G., Reitner, J.M., 2023. Chapter 20 - the Alps: glacial landforms during the deglaciation (18.9–14.6 ka). In: Palacios, D., Hughes, P.D., García-Ruiz, J. M., Andrés, N. (Eds.), European Glacial Landscapes. Elsevier, pp. 175–183. https://doi.org/10.1016/B978-0-323-91899-2.00005-X.
Kelly, M.A., Buoncristiani, J.F., Schluechter, C., 2004. A reconstruction of the last glacial maximum (LGM) ice-surface geometry in the western Swiss Alps and contiguous Alpine regions in Italy and France. Eclogae Geol. Helv. 97, 57–75. https://doi.org/10.1007/s00015-004-1109-6.
Kerschner, H., Kaser, G., Sailer, R., 2000. Alpine Younger Dryas glaciers as palaeo-precipitation gauges. Ann. Glaciol. 31, 80–84. https://doi.org/10.3189/172756400781820237.
Li, Y., 2018. Determining topographic shielding from digital elevation models for cosmogenic nuclide analysis: a GIS model for discrete sample sites. J. Mt. Sci. 15, 939–947. https://doi.org/10.1007/s11629-018-4895-4.
Lukas, S., 2007. Early-Holocene glacier fluctuations in Krundalen, south central Norway: palaeoglacier dynamics and palaeoclimate. The Holocene 17, 585–598. https://doi.org/10.1177/0959683607078983.
Marchetti, M., Ghinoi, A., Soldati, M., 2017. The dolomite landscape of the Alta Badia (Northeastern Alps): a remarkable record of geological and geomorphological history. In: Soldati, M., Marchetti, M. (Eds.), Landscapes and Landforms of Italy. Springer International Publishing, Cham, pp. 123–134. https://doi.org/10.1007/978-3-319-26194-2_10.
Marcott, S.A., Shakun, J.D., Clark, P.U., Mix, A.C., 2013. A reconstruction of regional and global temperature for the past 11,300 years. Science 339, 1198–1201. https://doi.org/10.1126/science.1228026.
Marrero, S.M., Phillips, F.M., Caffee, M.W., Gosse, J.C., 2016. CRONUS-Earth cosmogenic 36Cl calibration. Quaternary Geochronology 31, 199–219. https://doi.org/10.1016/j.quageo.2015.10.002.
Monegato, G., Scardia, G., Hajdas, I., Rizzini, F., Piccin, A., 2017. The Alpine LGM in the boreal ice-sheets game. Sci. Rep. 7, 2078. https://doi.org/10.1038/s41598-017-02148-7.
Mutschlechner, G., 1932. Geologie der St. Vigiler Dolomiten: mit 1 geologischen Karte von G. Mutschlechner und P.Maibaur. Jahrbuch der Geologischen Bundesanstalt 82, 163–273.
Mutschlechner, G., 1933. Geologie des Gebietes zwischen St. Cassian und Buchenstein: (Südtiroler Dolomiten). Jahrb. Geol. Bundesanst. 83, 199–232.
Oien, R.P., Rea, B.R., Spagnolo, M., Barr, I.D., Bingham, R.G., 2022. Testing the area–altitude balance ratio (AABR) and accumulation–area ratio (AAR) methods of calculating glacier equilibrium-line altitudes. J. Glaciol. 68, 357–368. https://doi.org/10.1017/jog.2021.100.
Osmaston, H., 2005. Estimates of glacier equilibrium line altitudes by the Area x Altitude, the Area x Altitude Balance Ratio and the Area x Altitude Balance Index methods and their validation. Quat. Int. 138–139, 22–31. https://doi.org/10.1016/j.quaint.2005.02.004.
Paillard, D., 2009. Last Glacial Termination. In: Gornitz, V. (Ed.), Encyclopedia of Paleoclimatology and Ancient Environments. Springer, Netherlands, Dordrecht, pp. 495–498. https://doi.org/10.1007/978-1-4020-4411-3_123.
Panizza, M., 1973. Glacio pressure implications in the production of landslides in the dolomitic area. Geologia Applicata e Idrogeologia 3, 289–297.
Panizza, M., Corsini, A., Ghinoi, A., Marchetti, M., Pasuto, A., Soldati, M., 2011. Explanatory notes of the geomorphological map of the Alta Badia valley (Dolomites, Italy). Geogr. Fis. Din. Quat. 34, 105–126. https://doi.org/10.4461/GFDQ.2011.34.12.
Peel, M.C., Finlayson, B.L., McMahon, T.A., 2007. Updated world map of the Köppen-Geiger climate classification. Hydrol. Earth Syst. Sci. 11, 1633–1644. https://doi.org/10.5194/hess-11-1633-2007.
Pellitero, R., Rea, B.R., Spagnolo, M., Bakke, J., Ivy-Ochs, S., Frew, C.R., Hughes, P., Ribolini, A., Lukas, S., Renssen, H., 2016. GlaRe, a GIS tool to reconstruct the 3D surface of palaeoglaciers. Comput. Geosci. 94, 77–85. https://doi.org/10.1016/j.cageo.2016.06.008.
Penck, A., Brückner, E., 1909. Die Alpen im Eiszeitalter. Tauchnitz, Leipzig.
Piacentini, D., Troiani, F., Soldati, M., Notarnicola, C., Savelli, D., Schneiderbauer, S., Strada, C., 2012. Statistical analysis for assessing shallow-landslide susceptibility in South Tyrol (south-eastern Alps, Italy). Geomorphology 151, 196–206. https://doi.org/10.1016/j.geomorph.2012.02.003.
Porter, S.C., 1975. Equilibrium-line altitudes of late Quaternary glaciers in the Southern Alps, New Zealand. Quatern. Res. 5, 27–47.
Porter, S.C., 2000. Snowline depression in the tropics during the Last Glaciation. Quaternary Science Reviews 20, 1067–1091. https://doi.org/10.1016/S0277-3791(00)00178-5.
Porter, S.C., Orombelli, G., 1982. Late-glacial ice advances in the western Italian Alps. Boreas 11, 125–140.
Preusser, F., Graf, H.R., Keller, O., Krayss, E., Schlüchter, C., 2011. Quaternary glaciation history of northern Switzerland. E&G Quaternary Science Journal 60, 282–305. https://doi.org/10.3285/eg.60.2-3.06.
Rasmussen, S.O., Bigler, M., Blockley, S.P., Blunier, T., Buchardt, S.L., Clausen, H.B., Cvijanovic, I., Dahl-Jensen, D., Johnsen, S.J., Fischer, H., Gkinis, V., Guillevic, M., Hoek, W.Z., Lowe, J.J., Pedro, J.B., Popp, T., Seierstad, I.K., Steffensen, J.P., Svensson, A.M., Vallelonga, P., Vinther, B.M., Walker, M.J.C., Wheatley, J.J., Winstrup, M., 2014. A stratigraphic framework for abrupt climatic changes during the Last Glacial period based on three synchronized Greenland ice-core records: refining and extending the INTIMATE event stratigraphy. In: Quaternary Science Reviews, Dating, Synthesis, and Interpretation of Palaeoclimatic Records and Model-data Integration: Advances of the INTIMATE project (INTegration of Ice core, Marine and TErrestrial records, COST Action ES0907), vol. 106, pp. 14–28. https://doi.org/10.1016/j.quascirev.2014.09.007.
Rea, B.R., 2009. Defining modern day Area-Altitude Balance Ratios (AABRs) and their use in glacier-climate reconstructions. Quaternary Science Reviews 28, 237–248. https://doi.org/10.1016/j.quascirev.2008.10.011.
Reimer, P.J., Austin, W.E.N., Bard, E., Bayliss, A., Blackwell, P.G., Bronk Ramsey, C., Butzin, M., Cheng, H., Edwards, R.L., Friedrich, M., Grootes, P.M., Guilderson, T.P., Hajdas, I., Heaton, T.J., Hogg, A.G., Hughen, K.A., Kromer, B., Manning, S.W., Muscheler, R., Palmer, J.G., Pearson, C., Van Der Plicht, J., Reimer, R.W., Richards, D.A., Scott, E.M., Southon, J.R., Turney, C.S.M., Wacker, L., Adolphi, F., Büntgen, U., Capano, M., Fahrni, S.M., Fogtmann-Schulz, A., Friedrich, R., Köhler, P., Kudsk, S., Miyake, F., Olsen, J., Reinig, F., Sakamoto, M., Sookdeo, A., Talamo, S., 2020. The IntCal20 Northern Hemisphere radiocarbon age calibration curve (0–55 cal kBP). Radiocarbon 62, 725–757. https://doi.org/10.1017/RDC.2020.41.
Reitner, J.M., Ivy-Ochs, S., Drescher-Schneider, R., Hajdas, I., Linner, M., 2016. Reconsidering the current stratigraphy of the Alpine Lateglacial: implications of the sedimentary and morphological record of the Lienz area (Tyrol/Austria). E&G Quaternary Science Journal 65, 113–144. https://doi.org/10.3285/eg.65.2.02.
Rossato, S., Mozzi, P., 2016. Inferring LGM sedimentary and climatic changes in the southern Eastern Alps foreland through the analysis of a 14C ages database (Brenta megafan, Italy). Quaternary Science Reviews 148, 115–127. https://doi.org/10.1016/j.quascirev.2016.07.013.
Scapozza, C., Castelletti, C., Soma, L., Dall'Agnolo, S., Ambrosi, C., 2014. Timing of LGM and deglaciation in the Southern Swiss Alps. Geomorphologie: Relief, Processus, Environnement 20, 307–322. https://doi.org/10.4000/geomorphologie.10753.
Schimmelpfennig, I., Benedetti, L., Finkel, R., Pik, R., Blard, P.-H., Bourlès, D., Burnard, P., Williams, A., 2009. Sources of in-situ 36Cl in basaltic rocks. Implications for calibration of production rates. Quat. Geochronol. 4, 441–461. https://doi.org/10.1016/j.quageo.2009.06.003.
Schimmelpfennig, I., Benedetti, L., Garreta, V., Pik, R., Blard, P.-H., Burnard, P., Bourlès, D., Finkel, R., Ammon, K., Dunai, T., 2011. Calibration of cosmogenic 36Cl production rates from Ca and K spallation in lava flows from Mt. Etna (38°N, Italy) and Payun Matru (36°S, Argentina). Geochim. Cosmochim. Acta 75, 2611–2632. https://doi.org/10.1016/j.gca.2011.02.013.
Schlagenhauf, A., Gaudemer, Y., Benedetti, L., Manighetti, I., Palumbo, L., Schimmelpfennig, I., Finkel, R., Pou, K., 2010. Using in situ Chlorine-36 cosmonuclide to recover past earthquake histories on limestone normal fault scarps: a reappraisal of methodology and interpretations: using 36Cl to recover past earthquakes. Geophys. J. Int. 182, 36–72. https://doi.org/10.1111/j.1365-246X.2010.04622.x.

Servizio Geologico d'Italia, 1977. Foglio 028 "La Marmolada". Carta Geologica d'Italia alla scala 1:50.000.
Soldati, M., 2010. Dolomites: the spectacular landscape of the 'Pale Mountains'. In: Migon, P. (Ed.), Geomorphological Landscapes of the World. Springer Netherlands, Dordrecht, pp. 191–199. https://doi.org/10.1007/978-90-481-3055-9_20.
Soldati, M., Borgatti, L., 2009. Paleoclimatic significance of Holocene slope instability in the Dolomites (Italy). Geogr. Fis. Din. Quat. 32, 83–88.
Soldati, M., Corsini, A., Pasuto, A., 2004. Landslides and climate change in the Italian Dolomites since the Lateglacial. Catena 55, 141–161. https://doi.org/10.1016/S0341-8162(03)00113-9.
Soldati, M., Borgatti, L., Cavallin, A., De Amicis, M., Frigerio, S., Giardino, M., Mortara, G., Pellegrini, G.B., Ravazzi, C., Surian, N., 2006. Geomorphological evolution of slopes and climate changes in Northern Italy during the Late Quaternary: spatial and temporal distribution of landslides and landscape sensitivity implications. Geogr. Fis. Din. Quat. 29, 165–183.
Stansell, N.D., Polissar, P.J., Abbott, M.B., 2007. Last glacial maximum equilibrium-line altitude and paleo-temperature reconstructions for the Cordillera de Mérida, Venezuelan Andes. Quatern. Res. 67, 115–127. https://doi.org/10.1016/j.yqres.2006.07.005.
Stone, J.O., 2000. Air pressure and cosmogenic isotope production. J. Geophys. Res. Solid Earth 105, 23753–23759. https://doi.org/10.1029/2000JB900181.
Stone, J.O., Allan, G.L., Fifield, L.K., Cresswell, R.G., 1996. Cosmogenic chlorine-36 from calcium spallation. Geochim. Cosmochim. Acta 60, 679–692. https://doi.org/10.1016/0016-7037(95)00429-7.
Vandelli, V., Ghinoi, A., Marchetti, M., Soldati, M., 2019. Discovery and dating of Pre-LGM deposits in a high catchment of the Dolomites (Italy): new insights on climate-related geomorphological processes during the Late Pleistocene. Geomorphology 332, 22–32. https://doi.org/10.1016/j.geomorph.2019.02.004.
Veneto Region, 2020. Geoportal of the Regione del Veneto [WWW Document]. URL. https://www.regione.veneto.it/web/ambiente-e-territorio/geoportale (accessed 8.22.24).
Wirsig, C., Zasadni, J., Christl, M., Akçar, N., Ivy-Ochs, S., 2016. Dating the onset of LGM ice surface lowering in the High Alps. Quat. Sci. Rev. 143, 37–50. https://doi.org/10.1016/j.quascirev.2016.05.001.